Three-Dimensional Imaging of Breast Calcifications

Andrew D.A. Maidment, Michael Albert, and Emily F. Conant

Thomas Jefferson University, Department of Radiology
111 South 11th Street, Philadelphia, PA 19107

ABSTRACT

Approximately 50% of breast cancers are detected on the basis of calcifications alone. Regrettably, the presence of such calcifications is non-specific; only 30% of biopsies based on suspicious calcifications are malignant. We have investigated three methods (limited view reconstruction (LVR), synthetic tomography and stereoscopy) for three-dimensional imaging and analysis of microcalcifications. Our aim is to increase specificity by more accurately distinguishing between calcifications indicative of benign and malignant breast lesions. We have demonstrated that 3-D imaging of calcifications is possible using an LVR technique that includes semi-automated segmentation, correlation, and reconstruction of the calcifications. A clinical study of the LVR method is ongoing in which 2-D film and digital images are compared to 3-D images. The images are evaluated using a rating of 1 to 5, where 1 = definitely benign, 5 = definitely malignant, and a score of 3 or higher requires biopsy. To date, 3 radiologists have evaluated the images of 44 patients for which biopsy results were available. The use of 2-D and 3-D digital images resulted in doubling the diagnostic accuracy from 36% to 77%. Comparison to other techniques (stereomammography and synthetic tomography) is ongoing. Additionally, a high resolution CT scanner for breast tissue specimens is under construction for comparison of the reconstructed images to a "gold standard."

Keywords: digital mammography, stereomammography, mammary calcifications, image acquisition, image reconstruction, image segmentation, linear tomosynthesis

1. INTRODUCTION

There is evidence that both the mortality and morbidity resulting from breast cancer can be reduced with early detection.[1-4] While many imaging modalities have been investigated for the diagnosis of breast cancer, film-screen mammography is currently the most sensitive modality available for the early detection of this disease.[5-8] In current clinical practice, both symptomatic and asymptomatic women have a two-view mammographic examination consisting of medio-lateral and cranio-caudad film images of each breast. If there is cause for suspicion, then additional film images are obtained, including "cone-down views" in which extra compression is applied to the suspicious region of the breast to obtain an image with less overlaying tissue, and "magnification views" in which the geometry of image acquisition is altered to magnify the suspicious region (increasing the image signal-to-noise ratio at the expense of dose). In spite of these additional procedures, such approaches often fail to clearly indicate or contraindicate malignancy. As a result, a large number of benign biopsies are performed. Approximately 1 in 4 biopsies will result in the detection of a cancer.[9] Benign biopsies represent a major expense and one of the largest deterrents to women entering a screening mammography program. A definitive, non-invasive method of distinguishing between benign and malignant breast lesions is essential.

The detection and differential diagnosis of subtle lesions using film-screen mammography is further hindered by technical limitations, including insufficient film latitude, film granularity noise, and dose-inefficient scatter rejection.[10] These technical limitations arise in part because the film serves as the detector, the image display device, and the image storage device. These limitations can be overcome with a digital imaging system because the processes of acquisition, display and storage are performed independently and can be optimized separately.[11] Unfortunately, full-field digital mammography will not be widely available for several years. Instead, we propose that the most rapid implementation of digital mammography in the clinic can occur as an adjuvant diagnostic tool to film-screen mammography. There are more than 1000 small field-of-view digital mammography imaging systems installed in the United States for use in digital-mammography-guided stereotactic biopsies. We believe that such digital mammographic units provide an enormous,

SPIE Vol. 3240 • 0277-786X/98/$10.00

readily available resource for performing diagnostic "work-ups". Such work-ups could range from the simple use of the digital image receptor for magnified or non-magnified views of suspicious lesions, to 3-D mammography.

It has been reported that 29% to 48% of nonpalpable carcinomas are visible on the basis of calcifications alone.[9,12-16] Calcifications are especially important as a sign of early breast cancer.[9,17,18] Although certain calcifications are pathognomonic of malignant or benign lesions, so that biopsy is definitely indicated or contraindicated, in other instances the appearance is indeterminate, suggesting the possibility of carcinoma to varying degrees. A review of the literature reveals 25% to 36% of biopsies for calcifications are malignant.[14,19-23] Thus, calcifications are sensitive but not specific cancer markers.

In a seminal work[24], Lanyi has shown that the determination of malignancy in mammography has failed, in part, due to the processes of projection and superimposition that occur when any 2-D image is produced of a 3-D object. The result is a loss of information regarding the structure and morphology of breast lesions. In 1988, Lanyi[24] advocated a 3-D morphologic analysis of breast calcifications to overcome these limitations and demonstrated the utility of this approach using a technique that required biopsy. We took heed of Dr. Lanyi's hypothesis and developed a method for imaging calcifications in 3-D (Refs. 25-27). In this paper, we describe two additional methods for imaging the breast in 3-D with particular attention to breast calcifications.

2. METHODOLOGIES FOR 3-D BREAST IMAGING

We have investigated three methods of imaging the breast in 3-D - stereoscopy, limited view reconstruction (LVR) and linear tomosynthesis. The largest overriding concern in acquiring 3-D images of the breast is the dose involved in acquiring the images. The low energies used in mammography, required to obtain adequate subject contrast, result in relatively high exposures (on the order of 1R per image for an average sized breast). This combined with the relatively high sensitivity of breast tissue to radiation ($w_T = 0.05$, Ref. 28), means that mammography is a moderately high dose imaging procedure. To simply increase the number of views of the breast to acquire 3-D images is not an option. Care must be exercised to reduce the exposure for each view when acquiring 3-D images. It is for this reason that computed tomography (CT) of the breast is not considered clinically viable. In the three approaches described below, we shall consider techniques which require an increasing number of constituent images to generate a 3-D image, but in each instance the constituent images can be obtained with progressively lower doses.

2.1. Stereoscopy

Most human observers perceive the world using a stereoscopic vision system. The eyes of the observer are separated by approximately 7 cm, and because of this they record slightly different images. This effect is enhanced when the object being viewed is held closer to the observer. This binocular disparity, incorporated with clues such as shading from different light sources, superposition of structures and *a priori* information concerning the objects allows the observer to determine the position of objects relative to one another in 3-D.

Figure 1: Digital stereotactic imaging system used to acquire the image data for 3-D rendition.

Stereopsis can be simulated when radiographing the breast by acquiring images that are separated by a small angle and then displayed so that each eye views a different image. In our institution, we acquire images separated by angles of 3° to 5°; the optimum angle has yet to be determined. The images are each acquired with a dose that is approximately 1/2 of that used normally. The images are acquired on a prone stereotactic breast biopsy system (Fischer MammoTest™, Denver, CO), fitted with a small field-of-view digital mammography detector (Fischer MammoVision™) that produces images which have a format of 1024 x 1024 pixels (see Fig. 1). Each pixel has a size of 48 mm, and is digitized as a 12 bit value. Images are acquired at the Thomas Jefferson University Breast Imaging Center.

The stereoscopic mages are displayed on a Sun UltraSparc-2 2170, with Creator 3-D graphics. The images are displayed stereoscopically by presenting the data alternately to the left and right eyes of observers wearing synchronized shuttered eyewear (CrystalEyes™, San Rafael, CA) at 112 Hz. Software for image display was written in C and C++ using OpenGL and X Windows.

2.2. Limited View Reconstruction

LVR was proposed by us to generate true 3-D images of breast calcifications, but without the high dose associated with conventional 3-D x-ray techniques such as CT. We still require relatively high dose projection images (comparable to the dose used in non-grid film-screen mammography) to allow detection of the smallest possible calcifications within each projection image, but the technique requires very few images (typically 3, maximum of 7). This technique is possible because the calcifications are reconstructed from segmented image data, and a binary image reconstruction technique is employed.

The 3-D reconstruction of the calcification images is performed in a number of steps, beginning with acquisition of a limited number of projection images of the breast. Next, the calcifications are segmented from the background of breast parenchyma. The shape, size and position of each calcification in each view are used to determine the correspondence of the calcifications between the views. The 3-D location of each calcification is determined geometrically, and the 3-D shape of each calcification is derived using a simulated annealing approach. Finally, the images are rendered in 3-D, and a morphologic analysis and mammographic differential diagnosis is performed.

As with stereoscopy, images are acquired on a prone stereotactic breast biopsy system at the Thomas Jefferson University Breast Imaging Center. The image acquisition geometry is illustrated in Figure 2, where an object (x,y,z) is shown being imaged with the x-ray tube at point Q_1, yielding a projection at (u_1,v). Similarly, when the x-ray tube is at point Q_2, the object is projected to (u_2,v). A simple transformation from (u_1,u_2,v) to (x,y,z) is required to determine the 3-D location of the object. In routine usage of the biopsy system, only 3 images are acquired (-15°, 0° and +15° relative to the perpendicular vector to the detector). In the clinical study discussed in Section 3.2, only two images were used (-15° and +15°). However, a larger number of views may be acquired to improve the reconstruction. We have examined reconstructions which have used up to seven views of the breast, acquired in 15° increments from -45° to +45° (a total of 90° apart). Each digital projection image of the breast is performed at a glandular dose of approximately 0.6 mGy. Thus, the glandular dose required to perform a 3-D study is between 1.8 mGy and 4.2 mGy, depending upon the number of views acquired. Since only a fraction of the glandular tissue is irradiated, the mean glandular dose will be lower.

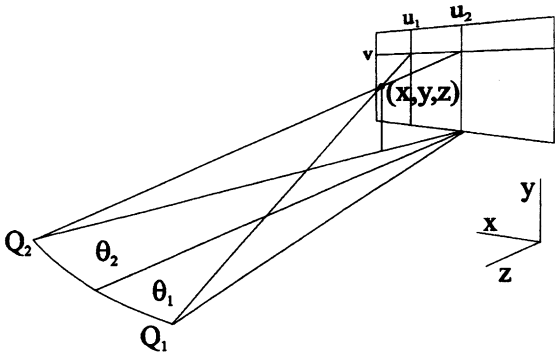

Figure 2: An illustration of the image acquisition geometry. When the x-ray tube is at position Q_1 the image of the calcification is projected onto the detector (dark gray) at a point (u_1,v), and at position Q_2 the image is projected to (u_2,v).

Currently, the calcifications in each image are identified manually. In this process, a human operator places a seed point near the center of a calcification. The calcification is then segmented semi-automatically using a recursive region-growing algorithm. Next, the corresponding projected image of the calcification is identified in the second view, and the calcification is segmented. These steps are repeated for every calcification for which correspondence between the views is found. This algorithm has been described in detail previously.[26,27]

It is possible to correlate the projected image of each calcification in the different views of the breast from the positions, shapes and sizes of the projected images. Note, for example, that the two projected positions $[(u_1, v)$ and $(u_2, v)]$ of a calcification at position (x,y,z) share a common coordinate, v, as shown in Figure 2. It is possible, therefore, to use the mass of the calcifications that span a similar range of v values to determine which projected shadow corresponds to which calcification in each view. By adding additional views, one can then verify the calculated 3-D position against the

segmented calcifications in those views, as well as identifying those calcifications, which are hidden or obscured in one or more of the other views. In this manner, it is possible to identify each calcification in each view.

We separately determine the *3-D location* and the *3-D shape* of each calcification. The 3-D location is determined geometrically. The 3-D shape of each calcification is determined using the segmented image data in conjunction with a simulated annealing reconstruction method. As illustrated in Figure 2, an object at point $C = (x,y,z)$ will produce a projection at $P_1 = (u_1,v)$ when viewed with the first x-ray source at point Q_1, and will produce a projection image at $P_2=(u_2,v)$ when viewed with the x-ray source at point Q_2. The line P_1Q_1 and P_2Q_2 lie in the plane Q_1Q_2C, and meet at the point C, which is the position of the calcification. These simple geometric considerations allow one to calculate the coordinates of C. A method for compensation of motion of the patient has also been developed.[29] When motion occurs, the lines P_1Q_1 and P_2Q_2 will not intersect. An affine transformation is determined by fitting the motion of obvious calcification pairs and then is applied to all calcifications being reconstructed.

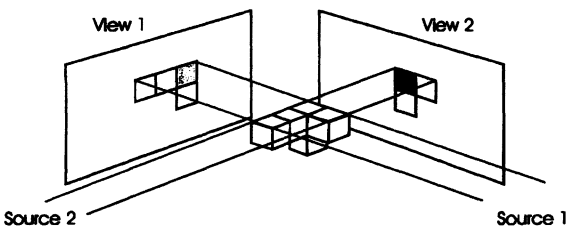

Figure 3: A simplified illustration of the reconstruction problem. An object (treated as a set of voxels containing calcium) is shown in two projections. Note that the intensity of the projection is related to the number of voxels traversed that contain calcium, and that the object is contained within the intersection of the back-projections (the image mask).

The intensity of the signal in each pixel of each view of the breast is dependent upon the amount of calcific material (and other breast tissues) in the path of the x-rays that contribute to signal at that pixel. This concept is illustrated in Figure 3, where a simulated object of equally attenuating cubes is held *in vacuo*, and imaged with an idealized imaging system in a non-divergent geometry. The intensity of the signal in the image depends upon the number of cubes traversed. To determine the 3-D shape of the object from the projection data requires an inverse transformation technique. We have chosen a simulated annealing method to which certain *a priori* constraints have been added. This method has also been described in detail previously.[26,27]

Once the list of voxels constituting the reconstruction of the calcification is obtained, the surface is approximated for the purpose of 3-D rendering using the marching cubes algorithm.[30] Rendering is performed using C and C++ with the OpenGL graphics library and X Windows. Objects are rendered in perspective with shading appropriate for both diffuse and specular reflection from both directional and diffuse light sources. The 3-D images may be viewed monoscopically or stereoscopically using CrystalEyes stereo eyewear.

2.3. Linear Tomosynthesis

In performing linear tomosynthesis, we again use our prone stereotactic biopsy system to acquire the projection image data set. For each tomosynthetic data set, fifteen images are acquired as the x-ray tube is moved through a 30 degrees arc; a clinically relevant geometry. As the x-ray focus is moved, the imaging plane **P** is held fixed. To perform a reconstruction, each x-ray image is viewed as a gray-scale function g_i defined on a region P_r of the imaging plane **P**, where i enumerates the x-ray exposure. For every plane **Q** parallel to **P** in which reconstruction will be performed, each projection position of the x-ray focus defines a one-to-one correspondence of points in the plane **Q** with the points in the plane **P**. Explicitly, for the i-th position of the x-ray tube, for each point q in **Q**, there is a line passing though the focus and q which meets **P** in a unique point p. Thus for every i there is a "projective" transformation between the points of **P** and **Q**. Further, the gray-scale function g_i on P_r can now be considered as a function g'_i defined in the region Q_i in the plane **Q**, and the value of the reconstructed gray scale image at a point q is the sum of all the g'_i which are defined at that point. As with conventional tomography, for objects lying within the plane **Q**, the functions g'_i add coherently to produce a well focused image, while for objects outside the plane are blurred. The advantage of synthetic tomography over conventional tomography is that the set of 15 or so images can be used to reconstruct multiple planes, while in conventional tomography each image would require an additional set of exposures.[31-33]

Typically we reconstruct the tomographic images in planar regions, Q_i, in 1 mm increments. These are rendered in X windows in a stack. One can use motion of the mouse to increment or decrement i thus allowing one to view the entire breast one slice at a time. It is also possible to window and level, and magnify the images.

3. RESULTS AND DISCUSSION

3.1. Stereoscopy

Stereoscopic images of the breast allow one to visualize the relative positions of objects in the breast. It is easier to appreciate this relationship in high contrast objects such as calcifications. In lower contrast objects, the relationship between the projections is less apparent. The method does allow one to understand how calcifications relate to the soft tissue stuctures of the breast.

We have found that it is more beneficial to render the constituent projection images of linear tomography data as stereoscopic pairs. In this way, you can view the breast at a variety of angles (typically covering 30° to 45° in 3° to 5° increments). Our viewing software allows us to double buffer stereoscopic images, and hence we can present smoothly rotating stereoscopic views of the breast. In this instance, the additional angular range of the image set allows one to determine with more confidence the relative relationship between different image features. Thus, an observer can build a better 3-D model of the breast in his or her mind. Unfortunately, there are dose considerations in using the linear tomographic projection data since these are typically acquired with a lower individual dose than true stereoscopic image pairs. The result is a lower SNR for any particular stereoscopic image pair, and hence the detection of certain objects such as very small calcifications will be adversely affected. We are currently evaluating this effect.

3.2. Limited View Reconstruction

3-D images of 44 cases of clustered calcification have been generated with the LVR method. Anecdotally, we have observed that in instances when the calcifications are associated with a mass, it has been possible to distinguish preferentially peripherally distributed calcifications from homogeneously distributed calcifications. This is possible in spite of the fact that in the 3-D renderings there is no frame of reference in which the reader can relate the calcifications to the mass. This observation is very important because preferentially peripherally distributed calcifications are predominately associated with benign diseases, while clustered malignant calcifications are more often homogeneously distributed. An example of a benign cluster of calcifications is shown in Figure 4. It has also been possible to elucidate the ductal distribution of some malignant calcifications using the 3-D reconstruction technique. An example of a malignant calcification cluster that demonstrates a ductal distribution is shown in Figure 5. In Figures 4 and 5, Figure a demonstrates a single digital mammographic views of the calcification cluster. The image depicts an area 2.5 cm x 2.5 cm. In Figures b and c, the calcifications that were segmented from each image are shown in two different views.

In our preliminary study of 44 cases, we compared the appearance of clustered calcifications in film-screen mammograms, digital 2-D mammograms and digital 3-D images. In the study, three radiologists separately reviewed each case. Fourteen of the cases were malignant, the remaining 30 cases were benign. In each case, the radiologist was asked to rate each case on a modified "degree of suspicion" scoring system; 5 = definitely malignant, 4 = probably malignant, 3 = suspicious for malignancy, 2 = probably benign, and 1 = definitely benign. A score of 3 or higher would indicate a biopsy procedure was necessary. With film images, the radiologist could use a magnifying glass or a hot-light if desired. In the case of the 2-D digital images, the readers were allowed to alter the display window and level and electronic magnification as desired. With the 3-D images, the radiologists could view the 3-D models from any angle.

The distribution of scores of the three radiologists is shown in Figure 6. As can be seen, the addition of the 2-D digital images and the 3-D images tended to shift the distribution of the benign scores lower, and the malignant scores higher. The accuracy of diagnosis rose from 36% for film to 63% adding 2-D digital images to 77% adding 3-D digital images; the latter representing a 210% improvement compared to film alone. The number of benign biopsies which would have been deemed necessary would have dropped from 28 for film alone to 16 using 2-D digital and 10 using 3-D data; a reduction of 66%.

3.3. Linear Tomosynthesis

We have not yet performed clinical linear tomosynthesis. Rather, the results of a preliminary phantom experiment are shown in Figure 7. The phantom consists of acrylic spheres contained in a water filled acrylic box. This box was superimposed upon a contrast-detail phantom. In Figure 7 (upper left), a projection image is shown. This image demonstrates the overlaying "clutter" of the spheres and cubes and effectively obscures most of the features of the contrast

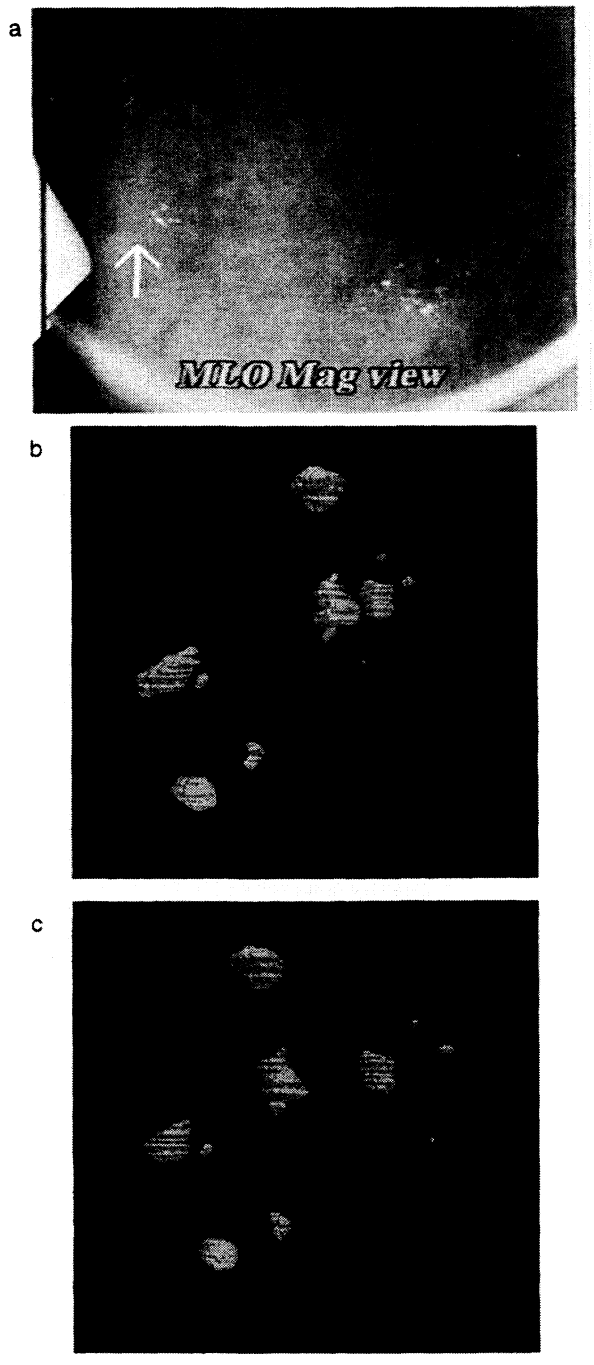

Figure 4: A radiograph of a benign cluster of calcifications (a). Also shown are 2 reconstructions of the cluster (b,c). The reconstructions show plate-like calcifications arranged in a spherical manner about a lucent center. This is typical of a fibroadenoma.

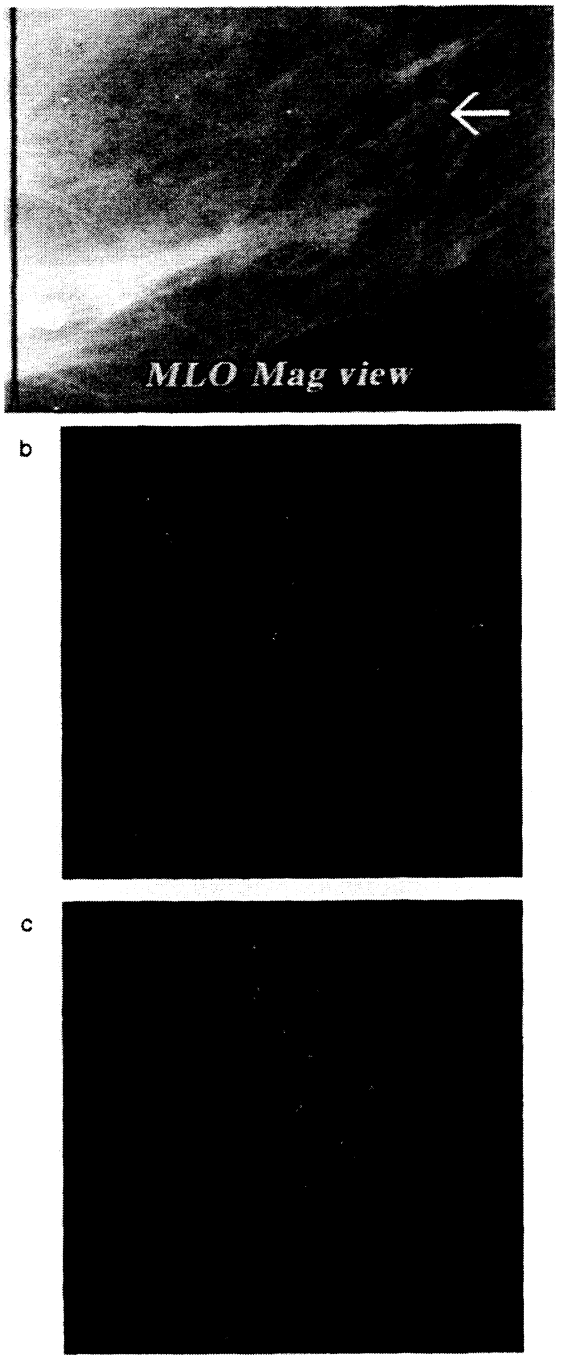

Figure 5: A radiograph of a malignant cluster of calcifications (a). Also shown are 2 reconstructions of the cluster (b,c). The reconstructions show a branching linear struction demonstrating ductal confinement of calcifications typical of a ductal carcinoma.

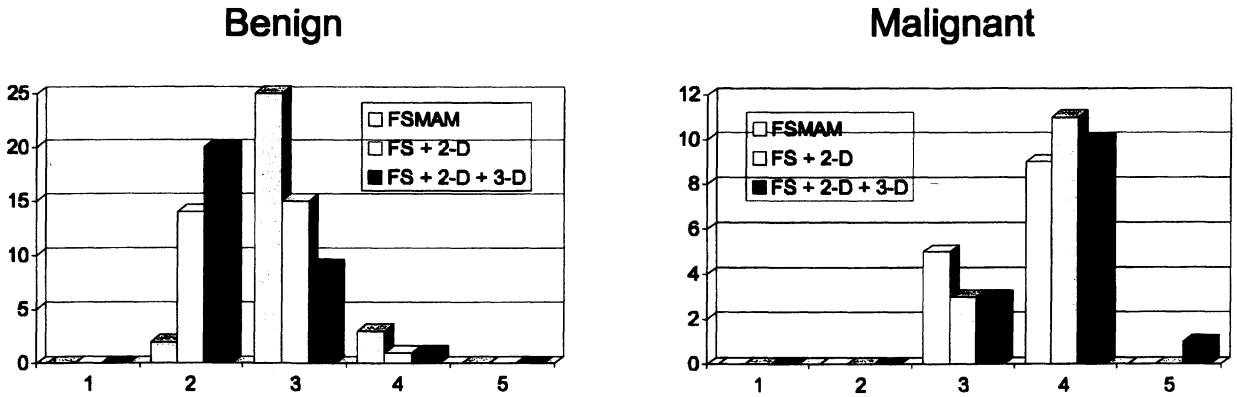

Figure 6: Histograms showing the number of benign and malignant cases rated with scores of 1 to 5. A score of 3 or greater would justify a biopsy.

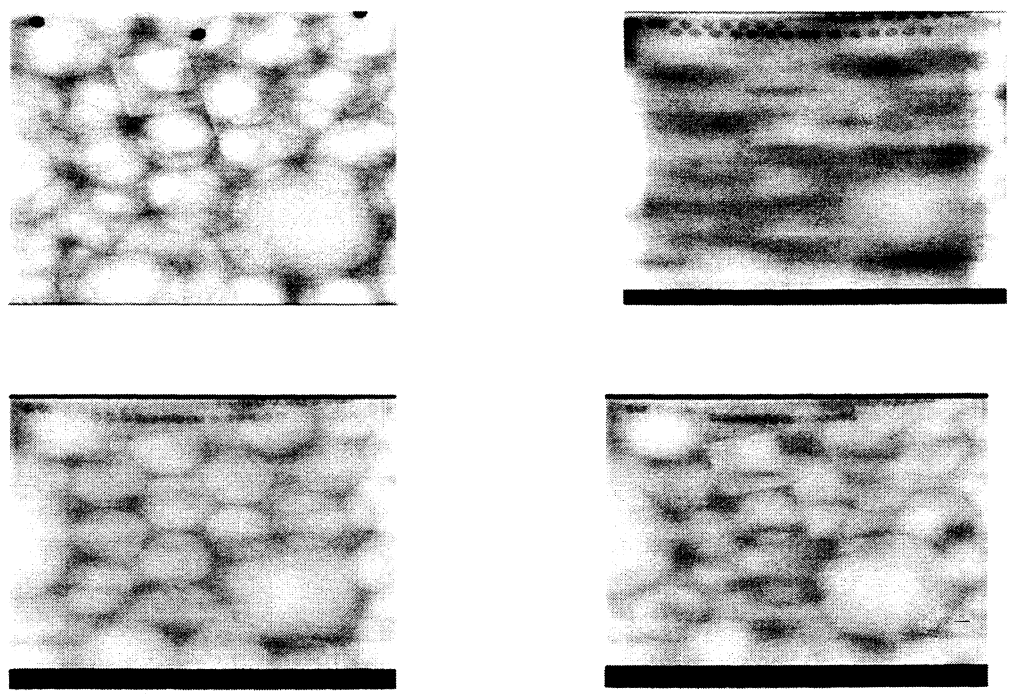

Figure 7: An tomosynthetic reconstruction of a phantom. The phantom consisted of a group of acrylic spheres and cubes immersed in water, and superimposed upon a contrast-detail phantom. A projection image is shown in the upper left. A slice through the contrast-detail phantom is shown in the upper right, clearly demonstrating more objects than are visible in the projection image. The lower images are reconstructed through slices which intersect the cubes and spheres.

detail phantom. Even at 10 times the dose this image was acquired at, we could not visualize more than 5 objects of the contrast-detail phantom. In Figure 7, we also show three reconstructions of the phantom. The lower images of Figure 7 are in the section containing the acrylic spheres. The upper right image of Figure 7, however, is in the plane containing the contrast-detail phantom. In this image, 24 contrast-detail elements are visible. The increase in detection of the objects is not related to the dose, but rather to the reduction in the overlaying clutter. Reduction of this structural noise results in an increase in the SNR of the contrast detail elements. It is hoped that similar improvements will be achieved by reducing the clutter of overlaying breast tissue and thus making subtle breast lesions more conspicuous.

4. CONCLUSIONS

In conclusion, we believe that existing digital mammography imaging systems should be used as an adjuvant tool to film-screen mammography. We have developed one such method that produces 3-D images of clustered mammary calcifications, and are investigating two more which place these calcifications in context with the surrounding tissues. These techniques use images that are acquired on a small field-of-view digital mammography prone stereotactic biopsy system. The LVR technique produces 3-D images using a method that includes identification, segmentation and correlation of each calcification in the breast in a limited number of projection images of the breast, and subsequent reconstruction of the calcifications from these views. Stereoscopic imaging of the breast requires fewer images but provides less depth perception. Linear tomosynthesis requires more images, but provides excellent depth perception, reducing overlaying clutter and making subtle lesions more conspicuous. The dose in each of these procedures is comparable to that used in magnification mammography. In a preliminary clinical evaluation, we have demonstrated that 3-D morphologic analysis of calcifications is possible and can significantly increase accuracy of diagnosis and decrease the number of benign biopsies required.

5. ACKNOWLEDGEMENTS

This research was supported by a grant from the RSNA Research and Education Fund, and is currently supported by the Department of Defense (DAMD17-96-1-6280 and DAMD17-97-1-7143). This work is conducted under the auspices of the International Digital Mammography Development Group. The authors wish to thank Dr. Stephen Feig, Dr. Catherine Piccoli, Dr. Steven Nussbaum, Dr. Elaine Wolk, and Ms. Lisa Fisher of Thomas Jefferson University for their assistance with this project.

6. REFERENCES

1. Seidman H *et al.* Survival experience in the Breast Cancer Detection Demonstration Project. *Ca.* **37**:258-290, 1987.
2. Feig SA. Decreased breast cancer mortality through mammographic screening: Results of clinical trials. *Radiology* **167**:659-665, 1988.
3. Shapiro *et al.* Current results of the breast cancer screening randomization trial: The Health Insurance Plan (HIP) of Greater New York, in NE Day and AB Miller (Eds) *Screening for Breast Cancer*, Toronto, Hogreofe, 1988.
4. Tabar L *et al.* Update of the Swedish two-county program for mammographic screening for breast cancer. *Radiol. Clin. N. Am.* **30**:187-210, 1992.
5. Kopans DB *et al.* Breast Imaging. *NEJM* **130**:960-967, 1984.
6. Sickles EA. Breast Imaging: A view from the present to the future. *Diagn. Imag. Clin. Med.* **54**:118-125, 1985.
7. Kopans DB. Non-mammographic breast imaging techniques. *Rad Clin N Am* **25**:961-971, 1987.
8. Kopans DB. Priorities for improved breast cancer imaging, in AG Haus and MJ Yaffe (eds) *Technical aspects of Breast Imaging*, RSNA, Oakbrook IL, 271-274, 1994.
9. Feig SA, Shaber GS, Patchefsky A, *et al.* Analysis of clinically occult and mammographically occult breast tumors. *AJR* 128:403-408, 1977.
10. Nishikawa RM *et al.* Scanned projection digital mammography. *Med Phys* **14**:717-727, 1987.
11. Maidment ADA. *Scanned-slot digital mammography*. PhD. Thesis, University of Toronto, Toronto, Canada, 1993.
12. Wolfe JN. Analysis of 462 breast carcinomas. *AJR* **121**: 846-853, 1974.
13. Frischbier H-J, Lohbeck HU. *Fruhdiagnostik des Mammakarzinoms*. Thieme, Stuttgart, 1977.

14. Bjurstam N. Radiology of the female breast and axilla. *Acta Radiol Suppl* **357, 1978**.
15. Menges V, Busing CM, Hirsch O. *RoFo* **135**:372-378, 1981.
16. Frankl G, Ackerman M. Xeromammography and 1200 breast cancers. *Radiol Clin North Am* **21**:81-91, 1983.
17. Moskowitz M. The predictive value of certain mammographic signs in screening for breast cancer. *Cancer* **51**:1007-1011, 1983.
18. Anderson I. Mammographic screening for breast carcinoma. Ph.D. Thesis , Malmo, 1980.
19. Murphy WA, DeSchryver-Kecskemeti K. Isolated clustered microcalcifications in the breast. *Radiology* **127**: 335-341, 1978.
20. Egan RL, McSweeney MB, Sewell CW. Intramammary calcifications without an associated mass in benign and malignant diseases. *Radiology* **137**:1-7, 1980.
21. Sickles EA. Further experience with microfocal spot magnification mammography in assessment of clustered breast microcalcifications. *Radiology* **137**:9-14, 1980.
22. Muir BB, Lamb J, Anderson TJ, *et al.* Microcalcification and its relationship to cancer of the breast. *Clin Radiol* **34**:193-200, 1983.
23. Sigfusson BF, Andersson I, Aspegren K, *et al.* Clustered breast calcifications. *Acta Radiologica* **24**: 273-281, 1983.
24. Lanyi M. *Diagnosis and Differential Diagnosis of Breast Calcifications.* Springer-Verlag, New York, 1988.
25. Robert N, Maidment ADA, and Yaffe MJ. Three-dimensional localization and display of breast microcalcifications. *Proceedings of the annual meeting division of medical and biological physics of the Canadian association of physics.* London Ontario, 1989.
26. Maidment ADA, Albert M, Conant EF and Feig SA. 3-D Mammary Calcification Reconstruction from a Limited Number of Views. *Proceedings of the SPIE*, **2708**, 378-389, 1996.
27. Maidment ADA, Conant EF, Feig SA, Piccoli CW and Albert M. Three-dimensional Analysis of Breast Calcifications in *Digital Mammography*, Excerpta Medica ICS-1119, Elsevier Sci., Holland, 245-250, 1996.
28. Limitation of Exposure to Ionizing Radiation. NCRP Report 116, Bethesda MD, 1993.
29. Albert M and Maidment ADA. Compensation for patient motion in stereotactic mammography. *Med. Phys.* **23** 1107, 1996.
30. Lorensen WE and Cline HE. Marching cubes: A high resolution 3D surface construction algorithm. *ACM Computer Graphics* **21**:163-169 1987.
42. Miller, E.R., McCurry, E.M., Hruka, B., An Infinite Number of Laminograms from a Finite Number of Radiographs, *Radiology*, 1971, 98 (249-255)
43. Grant, D.G. Tomosynthesis: a three dimensional radiographic imaging technique. *IEEE Trans. Biomed. Eng.*, 1972, 19 (20-28)
44. Ziedes des Plantes BG, Eine neue Methode zur Differenzierung in der Reontgenograpie (Panigraphie), *Acta. Radiol.* 1932, 13; 182-192 [Ger].